applied optics

Graphene-based bidirectional radiative thermal transfer method for heat engines

Alireza Nojeh,[1,3] George A. Sawatzky,[2,3] and Lorne A. Whitehead[2,*]

[1]Department of Electrical and Computer Engineering, University of British Columbia, Vancouver, British Columbia V6T 1Z4, Canada
[2]Department of Physics and Astronomy, University of British Columbia, Vancouver, British Columbia V6T 1Z1, Canada
[3]Quantum Matter Institute, University of British Columbia, Vancouver, British Columbia V6T 1Z4, Canada
*Corresponding author: lorne.whitehead@ubc.ca

Received 3 December 2018; revised 15 January 2019; accepted 1 February 2019; posted 1 February 2019 (Doc. ID 353354); published 8 March 2019

We present a method for substantially enhancing the rate of heat transfer into and out of the working fluid of a heat engine, using bidirectional thermal radiation exchange between the external environment and many individual graphene layers that are dispersed and suspended within an inert gas. This hybrid working fluid has the unique composite property of high optical absorption/emission yet low specific heat. Consequently, it can heat and cool rapidly, enabling a much greater cycle frequency and a commensurate increase in specific power, in comparison to conventional closed-cycle heat engines for which the cycle frequency is limited by the use of slower, non-radiative, thermal transfer.

https://doi.org/10.1364/AO.58.002028

1. INTRODUCTION

Heat engines are ubiquitous in modern society. They span a wide range of sizes and shapes, and all involve inducing temperature variations in a working fluid, which translate into pressure variations and volume changes whereby thermal energy is in part converted into mechanical work. One of the key limitations of heat engines is the time required to transfer heat into and out of the gaseous working fluid, which is limited by the poor thermal conductivity of gases. Here, we first outline this problem for heat engines, and then introduce the potential benefits that would arise if it were possible to use thermal radiation transfer to both rapidly heat and rapidly cool a gaseous working fluid. We then introduce a design for a working fluid that enables such transfer—a gaseous suspension of graphene in an inert gas, designed to provide an optimal absorption path length for broadband thermal radiation, without substantially increasing the specific heat above that of the ideal gas itself. We demonstrate that this enables a much higher operating frequency, and commensurately higher power density than would otherwise be possible for a closed-cycle heat engine.

2. REVIEW OF THE THERMAL TRANSFER PROBLEM IN HEAT ENGINES

Before discussing the new approach to heat engine thermal power exchange, it will be helpful to briefly summarize the basic nature of the problem. Generally, a heat engine accepts thermal energy Q_h from a thermal reservoir having an absolute temperature T_h and applies most of it to a working fluid that performs net mechanical work W on an external system. The residual energy, $Q_c = Q_h - W$, is released as heat into a thermal reservoir at a lower temperature T_c.

Closed-cycle heat engines reuse the same working fluid in each cycle. Generally, there are two goals for such an engine:

(a) to maximize the efficiency of conversion of heat to mechanical work, e, as defined in Eq. (1):

$$e = \frac{W}{Q_h}, \tag{1}$$

(b) to maximize the specific power, P_s, which is the ratio of the average power of the engine to its mass, as in Eq. (2):

$$P_s = \frac{fW}{m} = \frac{feQ_h}{m}, \tag{2}$$

where f is the cycle frequency, and m is the mass of the engine.

Generally, the efficiency is intermediate between 0 and the theoretical maximum value shown in Eq. (3):

$$e_{max} = 1 - \frac{T_c}{T_h}. \tag{3}$$

This value can be achieved in the limit only as the cycle frequency $f \to 0$, and, according to Eq. (2), the specific power in that case also approaches 0, showing that goals (a) and (b) are not mutually compatible. As a result, there is an optimum cycle frequency f_{opt} that yields the maximum specific power for a given heat engine. This can be calculated for a model Carnot engine that has thermal conductance values α and β between the working fluid and, respectively, the input

and output thermal reservoirs [1]. The answer is independent of α and β, and takes the form depicted in Eq. (4):

$$e_{\text{opt}} = 1 - \sqrt{\frac{T_c}{T_h}}. \tag{4}$$

At the optimum frequency, the specific power is given in Eq. (5) [2]:

$$P_{s_{\text{opt}}} = k\frac{\alpha\beta}{\sqrt{\alpha^2+\beta^2}}. \tag{5}$$

The value k depends on the details of the cycle. Equation (5) shows that, not surprisingly, the maximum specific power improves approximately in proportion to conductivities α and β. Therefore, it seems natural to design for the highest possible values for α and β, but that is difficult for gaseous working fluids. Gases have the advantage of large thermal expansivity, but they have very low thermal conductivity, effectively limiting α and β.

A common alternative is to abandon the closed thermodynamic cycle of the Carnot engine. For example, in steam engines and internal combustion engines, the input conductivity problem is avoided by injecting into a cylinder pre-heated steam or a combustible mixture that is then ignited. Further, they solve the output conductivity problem by discarding the working fluid from the cylinder with each cycle.

An alternate approach is used in the Stirling engine [3], wherein the working fluid is reused by cyclically forcing it through a regenerative heat exchanger in which the gas passes through narrow passages, minimizing the required thermal conduction distance and thus effectively increasing α and β. Unfortunately, the regenerator itself adds considerable mass and introduces aerodynamic drag, which reduces efficiency, so Stirling engines generally have relatively low specific power.

An alternative to increasing α and β could be to place throughout the working fluid a mesh of flexible highly thermally conductive fibers that would help to conduct heat into and out of the interior of the working fluid. However, it is readily shown that the heat capacity of the conductive fibers would greatly exceed that of the gas, so most of the heat passed into and out of the chamber would not actually be associated with heating and cooling the gas. Likely, such an arrangement would introduce mechanical losses as well. Here we present an alternative approach.

3. DIRECT BIDIRECTIONAL TRANSFER OF THERMAL RADIATION TO AND FROM AN INERT WORKING FLUID

We propose an alternate concept for more rapidly transferring heat into and out of the working fluid, by means of direct thermal radiation exchange between the environment and the working fluid. This is not practical with ordinary gases because they are substantially transparent to broadband thermal radiation. Of course radiative heat transfer has long been used to direct heat into (and in some cases out of) heat engines—often where direct solar radiation is plentiful and/or when radiation is the only means available for expelling waste heat. The new approach presented here is fundamentally different, whereby *the dominant heat transfer mechanism is bidirectional thermal radiation transfer directly between the external environment and the interior of the working fluid*. For this new approach to be practical, it is necessary for the absorption length for Planckian radiation corresponding to T_h to be on order of the diameter of the working fluid volume—if it is much shorter than that, the heat will not penetrate into the full volume, and, if much longer, little absorption will occur. We know of no practical gaseous working fluids that have this required broadband absorption characteristic. Previously, there has been interest in using lasers to heat gaseous heat engine working fluids having strong narrow-band absorption lines [4], but lasers are not very efficient, and, more importantly, the thermal emissivity of such narrow band absorbers is low, so radiative cooling, a required portion of the cycle, would be very slow. Instead, we propose an alternate hybrid working fluid for bidirectional thermal radiation transfer comprising a combination of an inert gas and a suspension of many separate graphene layers.

To understand the significance of graphene in this application, it is helpful to review the quantitative aspects of radiative cooling, which differs from the exponential decay of conductive cooling, since the intensity of Planckian radiation is proportional to the fourth power of temperature. To illustrate this, consider a thin slab of planar material of infinite extent, surrounded by vacuum, that is also free of electromagnetic radiation and therefore has a radiation temperature of 0 K. All cooling is via thermal radiation emitted from the slab's two surfaces. The slab has a specific heat per unit area $\tilde{C}_V$, and its emissivity is ε. Let $T(t)$ be the time-dependent temperature with $T(0) = T_o$. The radiated power per unit area, Q, is given by the Stefan–Boltzmann law in Eq. (6):

$$Q = 2\varepsilon\sigma T^4, \tag{6}$$

where the Stefan–Boltzmann constant $\sigma = 5.67\times10^{-8}\,\text{W m}^{-2}\text{K}^{-4}$, and the factor of 2 accounts for radiation leaving from both surfaces. To an approximation that is sufficient for the following analysis, the specific heat and emissivity can be modeled as being temperature invariant, and the temperature of the slab, at any given time, uniform. The rate of cooling is then given in Eq. (7):

$$\frac{dT}{dt} = -\frac{2\varepsilon\sigma}{\tilde{C}_V}T^4. \tag{7}$$

The decay form satisfying Eq. (7) is that of Eq. (8):

$$T = T_o\left(1+\frac{t}{\Delta}\right)^{-1/3}, \quad \text{where } \Delta = \frac{\tilde{C}_V}{6\varepsilon\sigma}T_o^{-3}. \tag{8}$$

The quantity Δ can be thought of as a characteristic time for radiative thermal decay. One way to interpret it is that when $t = 7\Delta$, $T = T_o/2$. It is interesting to calculate the characteristic time Δ in different scenarios. For example, consider a typical tungsten incandescent lamp filament with a thickness of 10^{-4} m and emissivity of 0.33 [5]. A slab with that thickness would have a value $\tilde{C}_V$ of $2.59\times10^2\ \text{J/m}^2\text{K}$, and at the typical operating temperature of 2,750 K, the characteristic time Δ given by Eq. (8) is 0.11 s, so it would cool to half its original temperature (i.e., to 1,375 K) in 0.77 s. (It should be pointed out that the above calculation is not exact because in general the ambient radiative environment is above absolute zero.

For example, in practice, it would often be around room temperature, approximately 300 K. However, this is not a consequential issue because the intensity of blackbody radiation varies in direct proportion to T^4. Thus, the incident thermal radiation would reduce the cooling speed in this example by only 0.014%. For simplicity, we omit this detail in the foregoing treatment).

Clearly, then, radiative cooling, even in this rather extreme case of a thin refractory material, is slow compared to the cycle times of most heat engines, which are typically roughly in the range from 5 ms to 50 ms. Likely, this is the reason that radiative cooling has never in the past played an important role in heat engines.

Consideration of graphene changes this: a single sheet of graphene [5] absorbs a fraction of about 0.023 of perpendicular incident light, and this absorption depends very weakly on incident direction or wavelength [6] . Therefore, the sheet has a broadband emissivity of about 0.023. It also has a $\bar{C}_V$ of about 1.5×10^{-3} J/m^{2}K at high temperatures [7]. At 2,750 K, the characteristic time Δ for radiative decay calculated using Eq. (8) is about 9×10^{-6} s. To summarize, a free graphene monolayer cools via thermal radiation about five orders of magnitude faster than a tungsten filament. Furthermore, despite the very low thickness of single graphene layers, their extreme tensile strength in the direction parallel to the sheet [8] makes it feasible for them to span the required macroscopic distances.

The selection of graphene for this purpose arises from our prior research [9,10] that investigated the radiative heating of carbon nanotube forests, for which the dominant absorption/radiation mechanisms are effectively those of graphene.

Figure 1 compares the exponential form of conductive thermal decay to the radiative thermal decay described in Eq. (8), with parameters selected so that each decays by ½ in unit time.

To make this concept more concrete, Fig. 2 depicts an approximate model for a hybrid working fluid consisting of multiple layers of single-sheet graphene in argon, separated

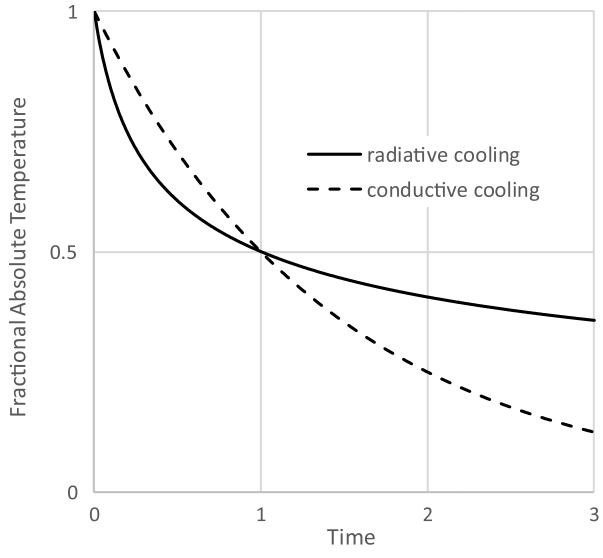

Fig. 1. Comparison of radiative and conductive thermal decay, with parameters adjusted so both decrease to 0.5 in unit time.

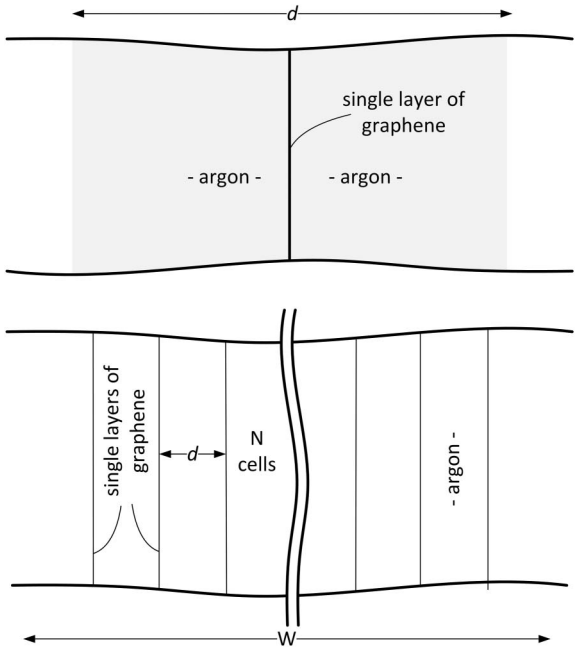

Fig. 2. Top: a single planar cell consisting of a single graphene sheet centered in an argon gas volume of width d. Bottom: an arrangement of N such cells, forming a total thickness of width $w = Nd$. Example values considered here are $d = 10$ micrometers, N = 100, and thus $w = 1$ mm.

by a distance, d, of 10 micrometers. There are 100 layers, so the overall thickness is 1 mm.

Despite the nano-scale thickness of graphene, sheets of macroscopic extent are known to be practical. For example, a variety of three-dimensional graphene structures can repeatedly expand and contract in response to external pressure [11].

Given the very low value of absorptivity (equal to emissivity of roughly 0.023), each graphene sheet is substantially transparent (97.7%), which means that, in the above multilayer structure, each sheet is able to substantially and independently exchange radiant heat (both incoming and outgoing radiation) with the thermal environment, with only minor involvement of the other layers. This idea is, to our knowledge, a critical new concept, which is responsible for the remarkable power density of this new form of heat engine.

We note that this is clearly an approximate calculation, because in principle there will be small amounts of interaction between the separate graphene sheets. However, even with many more proximate multilayers, the average amount of absorption per unit thickness changes little, so it is a reasonable approximation to model layers that are separated by 10 nm as independent [12].

A key concept for the hybrid working fluid is that its temperature should be substantially uniform, on the time scale of the planned thermodynamic cycle. This requires the thermal equilibration time between the graphene and the argon to be sufficiently short. This is easily calculated in this range of temperature, pressure, and size scale, for which there is negligible thermal convection, and the mean free path for the argon atoms is considerably less than d. In this regime, the thermal

equilibration time is reasonably accurately described by the thermal diffusion equation and is given approximately by Eq. (9):

$$\tau \cong \frac{s^2 \rho C_v}{k}, \tag{9}$$

where k, ρ, C_v are, respectively, the thermal conductivity, density, and specific heat of argon at $T = 300$ K and $P = 10^5$ Pa (1.79×10^{-2} W/mK, 1.607 kg/m^3, 3.13×10^2 J/kgK). (Here it is a reasonable approximation to use the bulk value for the thermal conductivity of argon because the mean free path is smaller than the spacing of the graphene layers, as shown next.)

For the dimensions in Fig. 1, the characteristic equilibration time τ given by Eq. (9) is 2.81×10^{-6} s. This surprisingly short time arises because d is small and raised to the power two. Because this time is much shorter than the radiative cooling time (which in the example below is 1000 times longer), it is a good approximation to simply model the argon and graphene as always being essentially equal in temperature.

The 100 layers of graphene contribute a heat capacity per unit area of 1.5×10^{-1} J/m^{2}K. The argon contributes a specific heat per unit area at constant volume of $\bar{C}_{va} = wC_{va} = 5 \times 10^{-1}$ J/m^{2}K, yielding a hybrid value of $\bar{C}_{vh} = 6.5 \times 10^{-1}$ J/m^{2}K. Similarly, the argon contributes a specific heat per unit area at constant pressure of $\bar{C}_{pa} = wC_{pa} = 8.33 \times 10^{-1}$ J/m^{2}K, yielding a hybrid value of $\bar{C}_{ph} = 9.83 \times 10^{-1}$ J/m^{2}K. Thus the specific heat ratio $\gamma = \bar{C}_{ph}/\bar{C}_{vh} = 1.513$, a value that is intermediate between that for a monotonic gas (1.67) and that for a diatomic gas (1.4), which is equivalent to a gas with about four degrees of freedom. This is mentioned here mainly to show that the presence of the dispersed graphene within the working fluid does not fundamentally alter the thermodynamic characteristics of the gas as a heat engine working fluid—but it does enable substantial direct thermal exchange with the environment. Of course this simple conceptual model is only approximate, but as in other idealized thermodynamic calculations (such as that for the Carnot cycle), it enables a helpful conceptual understanding of this system. In particular, it is instructive for calculating the efficiency of a simple thermal cycle. A cycle for this purpose traces the path in PV space shown in Fig. 3.

Using the standard formulas for adiabatic expansion and contraction, the values for the pressure P, the width w, and the temperature T for the four points in Fig. 3 are shown in Table 1.

The mechanical work input required for transition 1 to 2 is 277 J/m^2. Transition 2 to 3 requires a radiative heat input of 396 J/m^2. Transition 3 to 4 provides a mechanical work output of 396 J/m^2. Finally, the transition from 4 to 1 yields a radiative heat output of 277 J/m^2. The net output of work per cycle is 118 J/m^2, and thus the efficiency in this example is 30%. By design, the cycle time is dominated by transition 4 to 1, and can be calculated using Eq. (8): estimating the emissivity at 0.9, the radiative cooling transition requires 1.4 ms. The operating frequency is therefore 714 Hz, corresponding to an average mechanical output power of 85 kW/m^2.

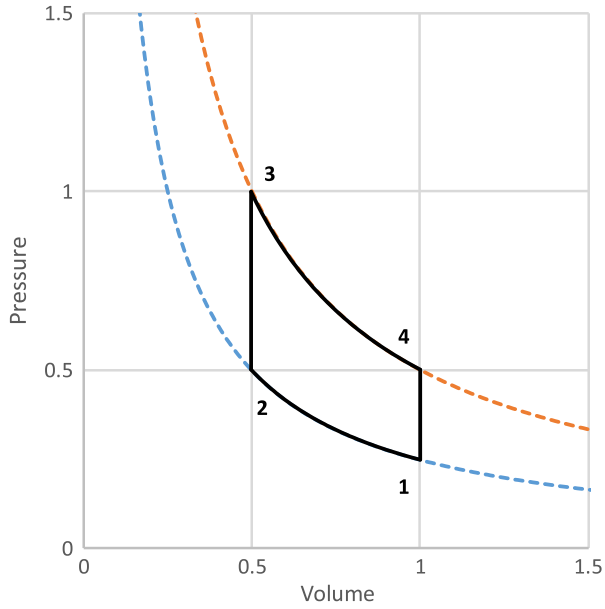

Fig. 3. Closed thermodynamic cycle in PV space. Transition 1 to 2 is rapid adiabatic compression, 2 to 3 is rapid radiative heating of the graphene, which heats the surrounding gas by thermal conduction, and 3 to 4 is rapid adiabatic expansion. The last transition, 4 to 1, comprises almost all of the cycle time, during which the hybrid working fluid cools by thermal conduction from the argon to the graphene layers, which in turn transmit the heat to the exterior via Planckian radiation.

Table 1. Four Cycle Points for an Example Radiative Transfer Heat Engine[a]

Point#	P (kPa)	w (mm)	T (K)	Q_{in} (J/m^2)	W_{out} (J/m^2)
1	333	1.0	1,000	0	−277
2	951	0.5	1,427	396	0
3	1,357	0.5	2,036	0	396
4	476	1.0	1,427	−277	0
Sum	-	-	-	118	118

[a]The columns Q_{in} and W_{out} refer to energy exchange during the transition from each cycle point to the next.

The mass per unit area of the hybrid working fluid is 1.45×10^{-3} kg/m^2 and likely negligible compared to the power coupling system. A simple coupling system could be a planar mass that resonates with the effective spring constant of the hybrid working gas, estimated in this case to require about 45 kg/m^2. (More sophisticated magnetic couplers might require significantly less mass.) Thus, the specific power could be 1.9 kW/kg or more. In comparison, the best specific power for Stirling engines [13] is about 0.3 W/kg, and many automotive internal combustion engines produce less than 1.9 kW/kg.

4. CONCLUSION

Generally, the concepts described above could be applied in a wide variety of size scales and geometries. One promising area could be muscle-like actuation in mobile robots. Another could

be autonomous aircraft, wherein sunlight would provide the radiant heat, enabling direct conversion of solar radiation to mechanical power for rotor systems. Since this is a new thermal transfer approach for heat engines, it is possible that the most interesting applications are yet to be determined. Finally, a note is in order as to the feasibility of the concept based on existing materials. While we have used aligned graphene sheets as the model material in order to simplify the analysis, the basic concept—that of a highly absorptive medium with low thermal mass based on an extremely porous nanostructure—is equally amenable to other embodiments, e.g., based on graphene sponges, large-scale sheets of carbon nanotubes [14], or even hybrid structures combining carbon nanotube networks and graphene layers [15]. The specific application of interest will determine the size scale of the engine, which will in turn dictate the choice of material to form the working fluid based on available technologies. For example, a miniature device might use ordered sheets of single-layer graphene, while a larger-scale device might require more robust and less ordered structures such as graphene–nanotube composites.

Funding. Natural Sciences and Engineering Research Council of Canada (NSERC) (RGPAS-2017507958, RGPIN-2017-04608); Canada Foundation for Innovation (CFI); British Columbia Knowledge Development Fund (BCKDF); Canada First Research Excellence Fund, Quantum Materials and Future Technologies Program.

REFERENCES

1. F. L. Curzon and B. Ahlborn, "Efficiency of a Carnot engine at maximum power output," Am. J. Phys. **43**, 22–24 (1975).
2. J. M. Gordon, "On optimized solar-driven heat engines," Sol. Energy **40**, 457–461 (1988).
3. J. Chen, "The effect of regenerative losses on the efficiency of a Stirling heat engine at maximum power output," Int. J. Ambient Energy **18**, 107–112 (1997).
4. M. Garbuny and M. J. Pechersky, "Laser engines operating by resonance absorption," Appl. Opt. **15**, 1141–1157 (1976).
5. Y. S. Touloukian, *Thermophysical Properties of Matter* (IFI/Plenum, 1970), Vol. **7**–Thermal Radiative Properties.
6. K. F. Mak, M. Y. Sfeir, Y. Wu, C. H. Lui, J. A. Misewich, and T. F. Heinz, "Measurement of the optical conductivity of graphene," Phys. Rev. Lett. **101**, 196405 (2008).
7. E. Pop, V. Varshney, and A. K. Roy, "Thermal properties of graphene: fundamentals and applications," MRS Bull. **37**(12), 1273–1281 (2012).
8. C. Lee, X. Wei, J. W. Kysar, and J. Hone, "Measurement of the elastic properties and intrinsic strength of monolayer graphene," Science **321**, 385–388 (2008).
9. P. Yaghoobi, M. V. Moghaddam, and A. Nojeh, "Heat trap: light-induced localized heating and thermionic electron emission from carbon nanotube arrays," Solid State Commun. **151**, 1105–1108 (2011).
10. M. V. Moghaddam, P. Yaghoobi, G. A. Sawatzky, and A. Nojeh, "Photon-impenetrable, electron-permeable: the carbon nanotube forest as a medium for multiphoton thermal-photoemission," ACS Nano **9**, 4064–4069 (2015).
11. H. Hu, Z. Zhao, W. Wan, Y. Gogotsi, and J. Qiu, "Ultralight and highly compressible graphene aerogels," Adv. Mater. **25**, 2219–2223 (2013).
12. G. Dovbeshko, V. Romanyuk, D. Pidgirnyi, V. Cherepanov, E. Andreev, V. Levin, P. Kuzhir, T. Kaplas, and Y. Svirko, "Optical properties of pyrolytic carbon films versus graphite and grapheme," Nano. Res. Lett. **10**, 234 (2015).
13. N. P. Nightingale, "Automotive Stirling engine: Mod II design report," Technical report DOE/NASA/0032-28, NASA CR-175106, MT186ASE58SR (1986).
14. L. Xiao, Z. Chen, C. Feng, L. Liu, Z. Q. Bai, Y. Wang, L. Qian, Y. Zhang, Q. Li, K. Jiang, and S. Fan, "Flexible, stretchable, transparent carbon nanotube thin film loudspeakers," Nano Lett. **8**, 4539–4545 (2008).
15. Z. Sui, Q. Meng, X. Zhang, R. Ma, and B. Cao, "Green synthesis of carbon nanotube-graphene hybrid aerogels and their use as versatile agents for water purification," J. Mater. Chem **22**, 8767 (2012).